



HAL
open science

Unexpected One-Pot Formation of Lactam Oximes from Amino-Hydroxamic Esters

Santiago Lascano, Arie van der Lee, Marie Lopez

► **To cite this version:**

Santiago Lascano, Arie van der Lee, Marie Lopez. Unexpected One-Pot Formation of Lactam Oximes from Amino-Hydroxamic Esters. *European Journal of Organic Chemistry*, 2022, 2022 (21), 10.1002/ejoc.202200102 . hal-03871396

HAL Id: hal-03871396

<https://hal.science/hal-03871396>

Submitted on 7 Dec 2022

HAL is a multi-disciplinary open access archive for the deposit and dissemination of scientific research documents, whether they are published or not. The documents may come from teaching and research institutions in France or abroad, or from public or private research centers.

L'archive ouverte pluridisciplinaire **HAL**, est destinée au dépôt et à la diffusion de documents scientifiques de niveau recherche, publiés ou non, émanant des établissements d'enseignement et de recherche français ou étrangers, des laboratoires publics ou privés.

Unexpected one-pot formation of lactam oximes from amino-hydroxamic esters

Santiago Lascano,^[a] Arie van der Lie,^[b] Marie Lopez*^[a]

[a] Institut des Biomolécules Max Mousseron (IBMM), CNRS, Université de Montpellier, ENSCM UMR 5247, 1919 route de Mende, 34293 Montpellier, France; * E-mail: marie.lopez@cns.fr

[b] IEM, Université de Montpellier, CNRS, ENSCM, Place E. Bataillon CC047, 34095 Montpellier, France

Abstract

Unexpected one-pot intramolecular formation of lactam oximes from the corresponding amino-hydroxamic ester in presence of amine is described. Several reaction parameters were studied and the importance of the base and the size of the resulting cycle were shown. This reaction, proceeding in high yield in described conditions, and can thus be considered as a new synthetic approach to prepare lactam oximes in a one-pot manner and in mild conditions.

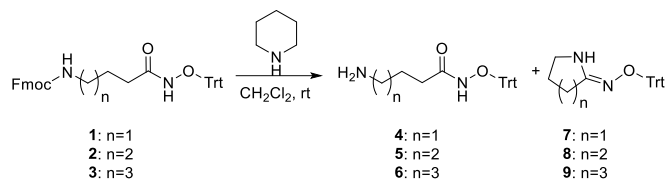
Introduction

In the context of our work on hydroxamic acids for medicinal chemistry purposes, we identified serendipitously a new synthesis pathway to prepare lactam oximes from easily accessible linear protected alkyl amino-hydroxamic acid derivatives. Several classes of lactam oximes were previously reported and mainly carbohydrate-based lactam oximes. For instance, such derivatives were shown of high interest for selective inhibition of Cex class of xylanases [1] and for α -amylase inhibition,[2] *e.g.* GIHL compound [3]. More recently, D-gluconhydroximo-1,5-lactam and its oxime substituted derivatives were described as potent chaperone of β -glucocerebrosidase in Gaucher disease. [1] Interestingly, glucolactam oxime was identified as transition-state mimic for glucosidases.[4] Synthesis of such carbohydrate-based lactam oximes, mainly proceeded through thiol derivatives and *via* carbohydrate synthesis methodology in more than 10-steps. Several lactam oximes other than carbohydrate were also described. Synthesis of lactam oxime from quinolinone, leading to 6- and 7-membered ring derivatives,[5] and from *N*-oxide pyridines [6] were also reported. Lactam oxime were also reported as potent HSP90 inhibitors.[7] Finally, an eleven-steps synthesis of lactam oxime squalene and its interest as squalene-hopene cyclase compare to amidoxime analogue was described.[8] Therefore, despite their potential interest, little is described about lactam oxime synthesis and reported synthesis occur in numerous steps or in harsh conditions. Thus, in this work, we reported a new synthesis pathway of lactam oximes derivatives and studied various synthesis parameters. Interestingly, we identified optimised conditions for 5-, 6- and 7-membered ring derivatives and obtained crystal structure for 5 and 6-membered ring derivatives, compounds 7 and 8, respectively.

Results and discussion

Synthesis

In our synthetic pathway to prepare enzymatic inhibitors bearing hydroxamic acid moieties, one step was a routine Fmoc deprotection of compounds **1-3** to the corresponding amines **4-6** with piperidine in dichloromethane (Scheme 1). However, isolated yields of the free amine were surprisingly low, in particular for amine **5**. LC-MS analysis of the reaction mixture showed an unidentified side-product in large amount for the deprotection of compound **2** and in lesser amount for deprotection of compounds **1** and **3**.



Scheme 1. Initial reaction conditions for Fmoc deprotection.

Formation of lactam oximes from the corresponding linear di-protected amino-hydroxamic acids is interesting as it is the only example, to our knowledge, of this kind of condensation reaction happening in a one-pot manner. The described formation of these compounds from an amino compound and a hydroxamic ester involves the use of harsh chlorinating reagents such as PCl_5 [9] or POCl_3 [10], while the condensation of a lactam with an alkoxyamine has been described with triethyloxonium tetrafluoroborate,[5] or by thionation,[11-12] both cases corresponding to a formal activation of the carbonyl. In order to facilitate the synthesis of lactam oxime derivatives, there is an interest of developing a two-step one-pot cyclisation of amino-hydroxamic esters and we decided to further investigate this unexpected reaction.

NMR analysis and X-ray crystal structures

To ascertain the identity of the side-product, compounds **7** and **8**, 5- and 6-membered rings, respectively, were isolated and characterised by NMR analysis. While ^1H NMR spectra of linear **5** and cyclic **8** were fairly similar, only displaying slight shifts, ^{13}C NMR spectra of cyclic compounds showed an important upfield shift of the quaternary sp^2 hydroxamate/lactam oxime carbon of around 20 ppm, consistent with a less electronegative nitrogen replacing the oxygen, resulting in a more shielded carbon (Figure S1). Finally, correlation of the protons at the end of the chain with the sp^2 carbon, was observed in the HMBC spectra of **8** (Figure 1) but absent in the case of **5** (Figure S2). This is a clear indication of the cyclic nature of compound **8**.

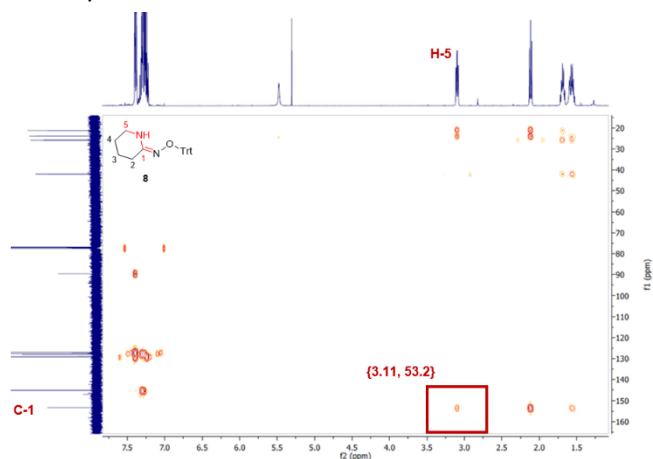
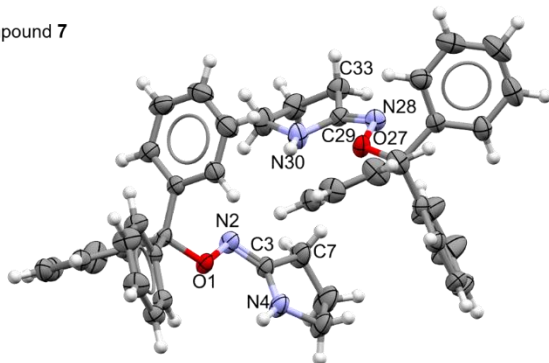


Figure 1. HMBC NMR analysis of cyclic compound (**8**) showing H-5/C-1 correlation.

To confirm the structure of compounds **7** and **8**, a lot of effort was put to obtain crystals for both cyclic derivatives **7** and **8** and their structures were definitely confirmed by the crystal structure (Figure 2 and 3). The 7-membered ring **9** was detected by LC-MS, but was produced in very low amounts and could not be isolated nor characterised.

Interestingly, x-ray crystal structure shows that exocyclic C-N bonds are shorter (1.289(2), 1.288(2) and 1.294(2) Å for **7** and **8** respectively) than endocyclic ones (1.345(2), 1.341(2) and 1.353(2) Å for **7** and **8** respectively), indicating that exocyclic C-N bond has a stronger double bond character. Intramolecular N-H...O distances (2.341, 2.288 and 2.160 Å for **7** and **8**, respectively) are consistent with weak hydrogen-bonding, but the torsion angles (-143.85/-179.15° and -167.02° for **7** and **8** respectively) seem to indicate that, at least in solid state, this bond is very weak (Table S1).

A- Compound **7**



B- Compound **8**

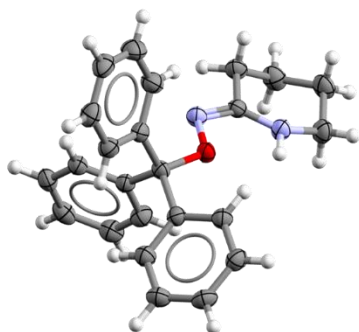


Figure 2. Molecular structure of compounds **7** (A) and **8** (B) in ORTEP-style. Atomic displacement ellipsoids have been drawn at 50% probability level. Atoms which are referenced to are labelled.

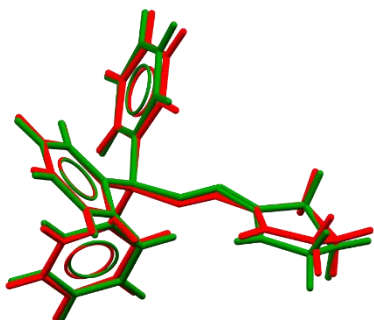


Figure 3. Best overlay of both independent molecules in the asymmetric part of the crystallographic unit cell of compound **7** structure. rmsd value is 0.1809 Å and maximum deviation 0.3918 Å. Both molecules are inversion-related in this view.

A standard geometry check against structures with similar fragments in the Cambridge Structural Database [13] using MOGUL program [14] shows that almost all bond distances, valence and torsion angles can be considered to be normal, except N2-C3-C7(122.53(1)°) and N28-C29-C33 (123.04(1)°) valence angles in the structure of **7** (Figure 2A).

These angles are considerably smaller than the one of similar fragments, approximately 130°, notably those with a similar pyrrolidine motif in the structure. Intramolecular N-H...O bonds seem to play an important role here in enlarging the N-C-C angles, since by enlarging the relevance criterion in the MOGUL query slightly a small cluster was found with similar fragments without pyrrolidine rings containing N-C-C angles close to those encountered in **7**, but with a neighbour oxy group similar to O1 and O27 in Figure 2A (see SI for more details). The structural cohesion in **7** originates from one weak intermolecular NH...N interaction (2.58(2) Å and \angle N-H...N=132.5(1) °) and a number of even weaker CH... π and NH... π interactions. Structure of **8** does not have any classical intermolecular hydrogen bond, and its structural cohesion appears to arise from very weak CH... π interactions only.

Influence of reaction conditions

After having ascertained the identity of the cyclic compounds, and in order to evaluate the influence of different parameters in the deprotection and cyclisation steps, the reaction was tested on analytical scale (typically around 2 mg of compound **2** in 1.2 ml of a 2:1 solvent/base mixture) and followed by LC-MS. The figures show the progression of the percentage of the cyclized compounds over the sum of cyclic and linear deprotected compound, as measured by the integration of the peaks obtained on the 214 nm UV chromatogram. Unless otherwise noted, reaction occurred from protected compound **2** to linear and cyclic compounds **5** and **8** (6-membered ring), respectively, solvent is dichloromethane, base is piperidine (~1200 equivalents), and temperature is 30 °C.

Influence of the solvent

A selection of solvents was tested, based on their polarity, proticity and miscibility with water, namely toluene, chloroform, dichloromethane (DCM), tetrahydrofuran (THF), methanol, acetonitrile and *N,N*-dimethylformamide (DMF) (Table 1). In all cases, the deprotection was complete in the first measurement, *i.e.* after 30 minutes and proportion of proportion of cyclic vs linear compounds over time was measured. The results are shown in Figure 4.

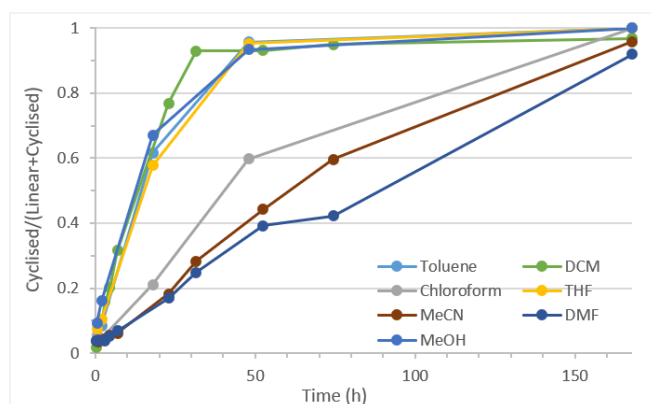


Figure 4. Solvent dependence of compound **5** cyclisation into compound **8**, in solvent/piperidine 2:1 v/v at 30 °C. Ratio of cyclic compound **8** over the sum of linear compound **5** and cyclic compound **8** is measured by HPLC analysis by peak integration on the 214 nm UV chromatogram.

Importantly, in all solvents full conversion was observed after 30 min. Regarding the cyclisation reaction, the slowest cyclisation rates were observed for DMF ($t_{50} \approx 90$ h), acetonitrile ($t_{50} \approx 60$ h) and chloroform ($t_{50} \approx 40$ h) with a linear kinetic. In DCM, methanol, toluene and THF, cyclisation rates were much faster with little effects of the solvents and t_{50} values varying from 12 h to 16 h.

Considering solvent parameters (Table 1), it appears that high dipole moment (μ) and high dielectric constant (ϵ) unfavoured cyclisation.

Table 1. Solvent properties

Solvent	Dipole moment μ (D) ^[a]	H-Bond donor	Relative polarity ^[b]	Dielectric constant ϵ (F·m ⁻¹) ^[c]
Dichloromethane	1.57	7.1	0.309	9.08
Methanol	1.71	22.3	0.762	33.1
Toluene	0.36	2.0	0.099	2.38
Tetrahydrofuran	1.75	8.0	0.210	7.47
Chloroform	1.01	5.7	0.259	4.81
Acetonitrile	3.92	6.1	0.460	37.5
Dimethylformamide	3.82	11.3	0.386	38.3

[a] ref. [15]; [b] ref. [16]; [c] ref. [17]

Influence of the temperature

Temperature-dependence experiments were carried out in DMF rather than in DCM in order to have access to a large range of temperature. This also gave more room for improvement in the cyclisation reaction. Reaction from **2** were carried out at 30 °C, 60 °C and 90 °C (Figure 5).

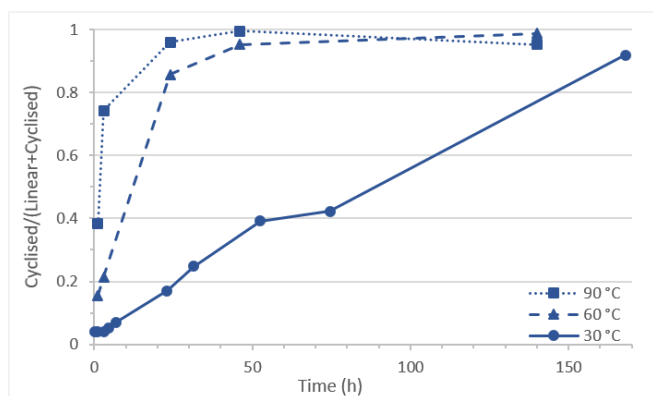


Figure 5. Temperature dependence of compound **5** cyclisation into compound **8**, in DMF/piperidine 2:1 v/v. Ratio of cyclic compound **8** over the sum of linear compound **5** and cyclic compound **8** is measured by HPLC analysis by peak integration on the 214 nm UV chromatogram.

Unsurprisingly, an increase of the temperature accelerates cyclisation rate. Increasing temperature from 30 °C to 60 °C strongly accelerate the reaction whereas almost no difference was observed between 60 °C and 90 °C. Therefore, in DMF, optimal temperature for cyclisation reaction is 60 °C.

Influence of the base

To study the impact of the base in deprotection and cyclisation reaction, a selection of cyclic, acyclic, secondary and tertiary nitrogenous bases, namely piperidine, morpholine, *N,N*-diisopropylethylamine (DIPEA), and *N,N*-diisopropylamine (DIPA), were selected. In order to avoid side-reactions from the dibenzofulvene side-product, inorganic bases and non-nucleophilic bases such as DBU were discarded. Unlike solvent and temperature, the choice of base has an important effect on the deprotection step (Figure 6).

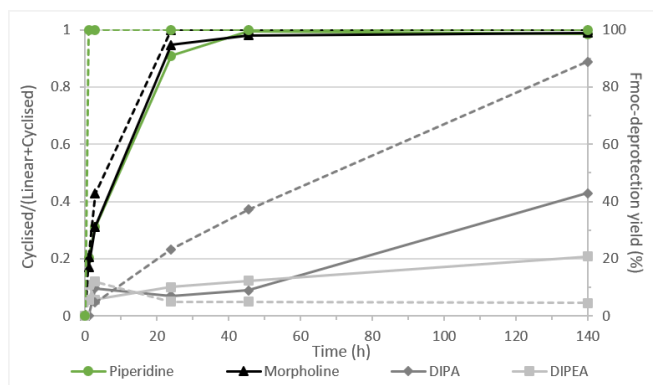
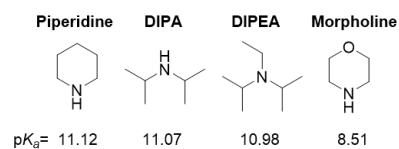


Figure 6. Base dependence of Fmoc-deprotection yield (dotted lines) and compound **5** cyclisation into **8** (plain curves), in DCM/base 2:1 v/v at 30 °C. Ratio of cyclic compound **8** over the sum of linear compound **5** and cyclic compound **8** as well as deprotection yield are measured by HPLC analysis by peak integration on the 214 nm UV chromatogram.

While piperidine leads to extremely fast reaction, with complete Fmoc deprotection under 30 min, morpholine leads to slightly longer reaction times and both DIPEA and DIPA lead to low amounts of deprotected compound **5** (Figure 6 dotted lines), which is consistent with literature.[18] Notably, regarding cyclisation kinetics (Figure 6 plain lines), it also depends on the base. With piperidine and morpholine fast cyclisation rates with similar kinetics were observed. Using DIPEA, cyclisation rate is low but considering the low deprotection yield, this might not be representative. However, interestingly, with DIPA, an initial



induction time was observed with low amount of cyclic compound until about 50 h before cyclisation actually occurred whereas the deprotection rate was regularly increasing up to 90%. Thus, aliphatic base used for the deprotection step has a crucial impact on this two-step one-pot reaction.

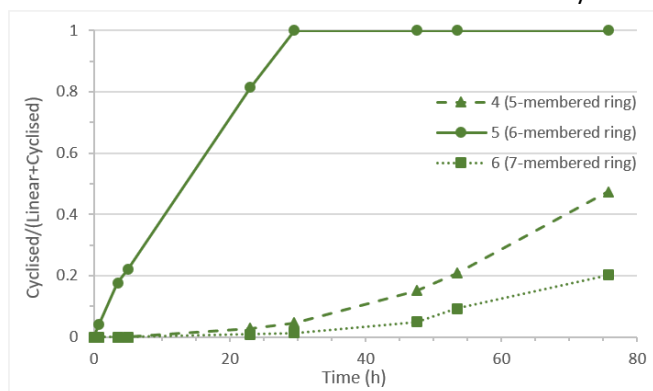
Figure 7. Structure and pK_a of aliphatic amines using for the two-step one-pot lactam oxime formation (from Broadwell tables).

Independently of the pK_a (Figure 7), a cyclic aliphatic base led to a higher deprotection yield and favour the cyclisation compare to non-cyclic bases that seems to hinder cyclisation.

Influence of the chain length

As mentioned previously, influence of chain length in cyclisation reaction was first observed when identifying the side-product, hypothesising that the formation of a cyclic compound could explain the differences for **7**, **8** and **9**. In order to quantify this difference, deprotection and cyclisation of compounds **1**, **2** and **3** were followed (Figure 8). As for the previous results using piperidine as a base, complete deprotection of **1-3** was observed after 30 min.

Figure 8. Ring-size dependence of the cyclization of **4-6** into **7-9**, in DCM/piperidine 2:1 v/v. Ratio of cyclic compounds **7-9** over the sum of linear **4-6** and **7-9** is measured by HPLC analysis by integration of peaks obtained on the 214 nm

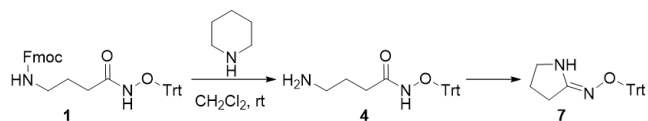


UV chromatogram.

Cyclisation rates of compounds **4-6** indicate very clearly that the 6-membered ring **8** is formed much faster ($t_{50} \approx 12$ h) than its 5- and 7-membered analogues compounds **7** and **9**, respectively with $t_{50} > 76$ h. This is obviously due to the higher stability of the 6-membered ring but very interestingly, these results showed that 5- and 7-membered lactam oximes can be obtained although after longer reaction time.

Cyclisation from starting from deprotected analogues

In order to decipher this one-pot deprotection/cyclisation synthesis and to better understand lactam oxime formation, we decided to follow the condensation starting directly from a Fmoc deprotected linear analogue. Compound **5** was first considered but its isolation proved to be particularly difficult, as it tended to readily cyclise to **8** during the purification steps. Therefore, in order to overcome this problem, and considering that a slower reaction is easier to follow, we decided to conduct these experiments starting from deprotected linear compound **4** (Scheme 2).



Scheme 2. Synthesis of lactam oxime **7** from Fmoc-deprotected amino-hydroxamic esters **4**.

Cyclisation of **4** was studied at 30 °C in dichloromethane, toluene, dichloromethane/piperidine 2:1, toluene/piperidine 2:1, as well as at 60°C in toluene and toluene/piperidine 2:1. The results are shown in Figure 9.

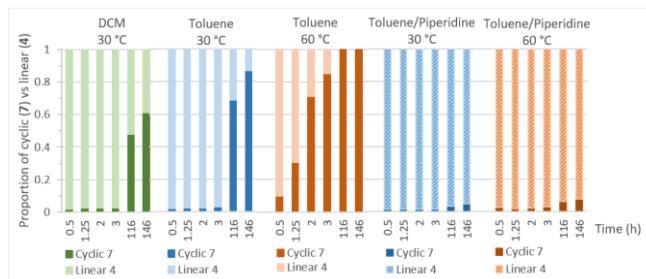
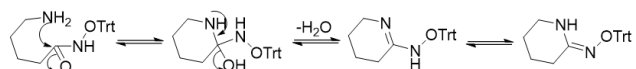


Figure 9. Temperature and base dependence of the cyclisation of Fmoc-deprotected linear compound **4**. Ratio of cyclic compounds **7** over the sum of linear compound **4** and cyclic compound **7** is calculated from HPLC analysis by peak integration on the 214 nm UV chromatogram.

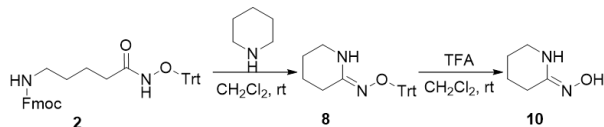
Starting from Fmoc-deprotected compound, cyclisation is slightly faster in toluene than in DCM. As in temperature dependence experiments for the cyclisation of **5** to **8** (Figure 5), results show that a higher temperature increases dramatically cyclisation rate with 85 % of cyclic compound **7** after 3 h in toluene at 60 °C compare to only 3 % at 30 °C. However, unexpectedly, the presence of piperidine do not lead to a higher cyclisation rate, but instead prevents the formation of cyclic analogue. This was also observed at higher temperatures, where the presence of piperidine led to 2 % of cyclisation after 2 h, instead of 71 % in toluene without base. Therefore, in the one-pot deprotection/cyclisation reaction, piperidine ensure the Fmoc deprotection but is not involved in the cyclisation step. A hypothesis for the cyclisation mechanism is presented Scheme 3 but is still to be confirmed.



Scheme 3. Mechanism hypothesis of α,ω -amino-trityl protected hydroxamic acid cyclisation.

Cyclisation yield

After studying these reaction parameters, we then selected the best identified conditions for the cyclisation (Scheme 4) and carried out the reaction on larger scale to prepare purified cyclic compound **8** in order to determine the yield of the overall reaction. Considering the available reactants, a 100 mg scale was used which is further representative of scales commonly used in medicinal chemistry program.



Scheme 4. Synthesis of lactam oxime **10** using one-pot deprotection cyclisation reaction.

This first trial, led to a surprisingly low yield of 38 %. We hypothesised that this low yield was linked to the presence of a highly apolar side-product, visible by LC-MS. Isolation of the unknown compound proved arduous and we could not come up with a satisfactory hypothesis for its structure, but we speculated that it was the result of the reaction of free dibenzofulvene – released from the reversible adduct formed with piperidine – with the trityl-protected hydroxamic acid. In order to circumvent this problem, the reaction was run in the presence of β -mercaptoethanol, as thiols are known to form more stable adducts with dibenzofulvene.[19-20] Deprotection and cyclization in dichloromethane/piperidine/ β -mercaptoethanol did indeed result in a higher yield of 54 %, which is an interesting

result to consider this reaction as a new way to access lactam oximes. Routine treatment of the resulting protected lactam oxime **8** in TFA in DCM yielded the corresponding deprotected lactam oxime **10** characterised by MS and NMR.

Conclusion

In conclusion a two-step one-pot synthesis for the preparation of trityl-protected lactam oximes was described. The study showed that for optimal conditions were the use of DCM, toluene, THF or methanol as solvent, with piperidine or morpholine and at 60 °C. Further deprotection of the trityl group can then be carried out using routine TFA in DCM to access lactam oximes.

Experimental Section

X-ray crystal structure. Crystal evaluation and data collection for **7** and **8** were performed on a Bruker Venture diffractometer with a microfocus Cu-K α source using the APEX3 [21] program. SAINT [21] was used for the integration of the data using default parameters, for the empirical absorption correction using spherical harmonics employing symmetry-equivalent and redundant data, and the correction for Lorentz and polarization effects. The crystal structure was solved using the *ab initio* iterative charge flipping method with parameters described elsewhere [22] using the SUPERFLIP program [23] and it was refined using full-matrix least-squares procedures on $|F|^2$ as implemented in CRYSTALS [24] on all independent reflections with $I > 3\sigma(I)$. The absolute structure for the non-centrosymmetric structure of **8** could not be determined reliably because of the absence of elements with sufficient anomalous scattering. The H atoms were all located in a difference map, but repositioned geometrically. They were initially refined with soft restraints on the bond lengths and angles to regularize their geometry (C---H in the range 0.93-0.98 Å) and $U_{\text{iso}}(\text{H})$ (in the range 1.2-1.5 times U_{eq} of the parent atom), after which the positions were refined with riding constraints.[25]

CCDC 2143586 (for Cpd **7**) and 2143587 (for Cpd **8**) contain the supplementary crystallographic data for this paper. These data can be obtained free of charge from The Cambridge Crystallographic Data Centre via www.ccdc.cam.ac.uk/structures.

General synthesis methods. Briefly, reagents for synthesis were purchased from Fluka, Sigma-Aldrich, and TCI, salts of the best grade available from Fluka or Sigma-Aldrich and used as received. Unless stated otherwise, flash chromatography was carried out Interchim PuriFlash 430 Instrument using 50 μm irregular silica cartridges (40-60 μm). Analytical TLC was performed on silica gel 60 F₂₅₄ (Merck). Analytical, reversed-phase HPLC was performed on a Thermo Scientific, UltiMate3000 system equipped with a C18 reversed-phase column (Thermo Scientific, Hypersil GOLD aQ, 2.1 x 50 mm, 1.9 μm) eluting with a linear gradient of MeCN in H₂O containing 0.1% formic acid at a flow rate of 0.5 ml.min⁻¹. ¹H and ¹³C NMR spectra were recorded on a Bruker 400 MHz spectrometer (Bruker DRX-400) and are reported as chemical shifts (δ) in ppm relative to (residual) solvent signal. Spin multiplicities are reported as a singlet (s), doublet (d), triplet (t), quartet (q), doublet of doublets (dd), doublet of quartets (dq) with coupling constants (J) given in Hz, or multiplet (m). ¹³C resonances were assigned with the aid of additional information from DEPT 135, HSQC and HMBC spectra. LCMS analyses were performed on an instrument equipped with a Shimadzu LC-20AD XR pump, SPD-M20A diode array detector. A C18 reversed-phase column (Phenomenex, Kinetex polar C18, 3 x 750 mm, 2.6 μm , 100 Å) was used. Elution was performed using a binary gradient (solvent A: H₂O + 0.1% formic acid; solvent B: ACN + 0.1% formic acid). Low resolution mass spectra were acquired using electrospray in positive and negative modes and are reported as mass-per-charge ratio m/z (intensity in %, [assignment]).

Compound 1. To a solution of **S4** (202 mg, 621 μmol), EDCI-HCl (178 mg, 927 μmol) and HOBt (98 mg, 730 μmol) in CH_2Cl_2 (15 ml) and DMF (5 ml), was added DIPEA (280 μl , 1.6 μmol) and then TrtONH₂ (213 mg, 772 μmol). The mixture was then left under stirring at rt overnight. The solution was then covered with water and extracted with CH_2Cl_2 . The organic fractions were collected, dried over Na_2SO_4 , filtered, and concentrated. Purification by flash column chromatography (SiO_2 , $\text{CH}_2\text{Cl}_2/\text{MeOH}$ 19:1) afforded compound **1** as a colourless solid (152 mg, 42%). ¹H NMR (400 MHz, CDCl_3 , *n/n*: stereoisomeric peaks): 8.24/8.00 (s, 1H), 7.80 (d, ³*J* (H,H) = 7.5, 2H), 7.65 – 7.57 (m, 2H), 7.56 – 7.48 (m, 3H), 7.43 (t, ³*J* (H,H) = 7.5, 2H), 7.40 – 7.30 (m, 14H), 5.05 – 4.62 (m, 1H), 4.47 – 4.36 (m, 2H), 4.30 – 4.18 (m, 1H), 3.12 – 2.83 (m, 2H), 1.93 – 1.43 (m, 4H); ¹³C NMR (101 MHz, CDCl_3) δ = 176.7 (C), 156.3 (C), 143.8 (C), 141.3 (C), 141.0 (C), 129.1 (CH), 128.2 (CH), 127.9 (CH), 127.7 (CH), 127.1 (CH), 125.1 (CH), 120.0 (CH), 93.5 (C), 66.4 (CH₂), 47.3 (CH), 40.5 (CH₂), 28.7 (CH₂), 23.2 (CH₂); *R_f* ($\text{CH}_2\text{Cl}_2/\text{MeOH}$ 9:1)= 0.68; ESI-MS *m/z*= 1187 [2M+Na]⁺, 605 [M+Na]⁺, 583 [M+H]⁺, 243 [Trt]⁺.

Compound 2. To a solution of **S5** (255 mg, 750 μmol), EDCI-HCl (143 mg, 750 μmol) and HOBt (144 mg, 1.07 mmol) in DMF (15 ml), was added TrtONH₂ (400 mg, 1.45 mmol). The mixture was then left under stirring at rt overnight. The solution was then covered with brine and extracted with CH_2Cl_2 . The organic fractions were collected, dried over Na_2SO_4 , filtered, and concentrated. Purification by flash column chromatography (SiO_2 , $\text{CH}_2\text{Cl}_2/\text{MeOH}$ 19:1) afforded compound **2** as a colourless solid (332 mg, 74%). ¹H NMR (400 MHz, CDCl_3) δ = 7.88 (s, 1H), 7.80 (d, ³*J* (H,H) = 7.5, 2H), 7.63 (d, ³*J* (H,H) = 7.5, 2H), 7.51 (s, 3H), 7.43 (t, ³*J* (H,H) = 7.5, 2H), 7.37 (s, 12H), 7.37 – 7.32 (m, 2H), 4.98 – 4.65 (m, 1H), 4.41 (s, 2H), 4.24 (s, 1H), 3.06 (s, 2H), 2.05 – 1.05 (m, 6H).; ¹³C NMR (101 MHz, CDCl_3) δ = 176.9 (C), 156.4 (C), 146.9 (C), 144.0 (C), 141.3 (C), 129.1 (CH), 128.2 (CH), 128.0 (CH), 127.3 (CH), 127.1 (CH), 125.0 (CH), 120.0 (CH), 93.5 (C), 66.5 (CH₂), 47.3 (CH), 40.5 (CH₂), 30.7 (CH₂), 29.2 (CH₂), 20.4 (CH₂). *R_f* ($\text{CH}_2\text{Cl}_2/\text{MeOH}$ 9:1)= 0.75; ESI-MS *m/z*= 619 [M+Na]⁺, 243 [Trt]⁺.

Compound 3. To a solution of **S6** (201 mg, 569 μmol), EDCI-HCl (164 mg, 855 μmol) and HOBt (88 mg, 648 μmol) in CH_2Cl_2 (15 ml) and DMF (5 ml), was added DIPEA (260 μl , 1.5 μmol) and then TrtONH₂ (198 mg, 719 μmol). The mixture was then left under stirring at rt overnight. The solution was then covered with water and extracted with CH_2Cl_2 . The organic fractions were collected, dried over Na_2SO_4 , filtered, and concentrated. Purification by flash column chromatography (SiO_2 , $\text{CH}_2\text{Cl}_2/\text{MeOH}$ 19:1) afforded compound **3** as a colourless solid (159 mg, 46%). ¹H NMR (400 MHz, CDCl_3) δ = 7.90 (s, 1H), 7.80 (d, ³*J* (H,H) = 7.4, 2H), 7.64 (d, ³*J* (H,H) = 7.4, 2H), 7.52 (s, 3H), 7.43 (t, ³*J* (H,H) = 7.4, 2H), 7.38 (s, 12H), 7.38 – 7.32 (m, 2H), 4.90 (s, 1H), 4.44 (d, ³*J* (H,H) = 6.8, 2H), 4.25 (t, ³*J* (H,H) = 6.8, 1H), 3.14 (s, 2H), 1.96 – 0.99 (m, 8H).; ¹³C NMR (101 MHz, CDCl_3) δ = 177.1 (C), 156.4 (C), 144.1 (C), 141.4 (C), 141.1 (C), 129.1 (CH), 128.2 (CH), 127.9 (CH), 127.7 (CH), 127.1 (CH), 125.1 (CH), 120.0 (CH), 93.4 (C), 66.5 (CH₂), 47.3 (CH), 40.8 (CH₂), 31.1 (CH₂), 29.5 (CH₂), 26.2 (CH₂), 23.0 (CH₂). *R_f* ($\text{CH}_2\text{Cl}_2/\text{MeOH}$ 9:1)= 0.77; ESI-MS *m/z*= 1243 [2M+Na]⁺, 633 [M+Na]⁺, 243 [Trt]⁺.

One-pot Fmoc-deprotection and cyclisation in analytical scale. Compound **1**, **2** or **3** (exactly *ca.* 2 mg) was solubilised in the appropriate solvent in LC-MS vial and selected base was added (1 ml final volume). Reaction mixture was incubated at appropriate temperature and was monitored overtime by LC-MS. Deprotection rate as well as proportion of cyclic vs. linear compounds were calculated from HPLC analysis by peak integration on the 214 nm UV chromatogram.

Compound 8. Compound **2** (101.5 mg, 178.2 μmol) was solubilised in DCM (6 ml). β -Mercaptoethanol (3 ml) and piperidine (3 ml) were added and the reaction mixture was stirred for 30 h at rt. Reaction mixture was diluted in DCM and washed with $\text{NH}_4\text{Cl}_{\text{sat}}$ ($\times 1$). Aqueous layer was back-extracted with DCM ($\times 2$), organic layers were combined, dried over Na_2SO_4 , filtered and concentrated under vacuum. Purification of the crude product by flash chromatography (2:3 EtOAc/hexane) afforded **8** (34,6 mg, 97.0 μmol) with 54% yield. ¹H NMR (400 MHz, CDCl_3): 7.42-7.39 (m, 6H), 7.33-7.23 (m, 9H), 3.11 (td, *J* = 1.6, 6 Hz, 2H), 2.14 (t, *J* = 6.4 Hz, 2H), 1.71 (m, 2H), 1.58 (m, 2H), 1.29 (s, 1H); ESI-MS *m/z*= 379 [M+Na]⁺.

Compound 10. Compound **8** (23.2 mg, 65.1 μmol) was solubilised in DCM (3 ml) and TFA (20 μl , 0.26 mmol) was added. Solution turned bright yellow and triisopropylsilane (TIPS), trityl scavenger, was added until disappearance of

the yellow colour. Crude mixture was washed with $\text{NH}_4\text{Cl}_{\text{sat}}$ ($\times 1$). Aqueous layer was back-extracted with DCM ($\times 2$), organic layers were combined, dried over Na_2SO_4 , filtered and concentrated under vacuum. Title compound **10** (3,7 mg, 32.4 μmol) was obtained with 50% yield. ^1H NMR (400 MHz, CDCl_3): 3.23 (t, $J = 8.0$ Hz, 1H), 2.27 (t, $J = 8.0$ Hz, 1H), 1.75 (m, 2H), 1.29-1.24 (m, 6H), 0.90-0.84 (m, 1H); ESI-MS $m/z = 115$ $[\text{M}+\text{H}]^+$.

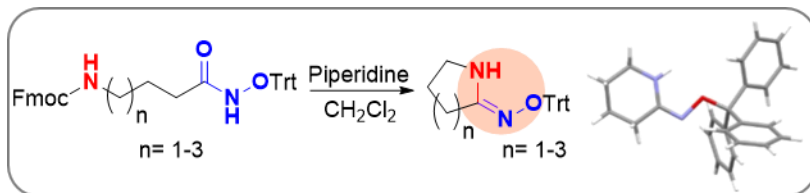
Acknowledgements

We thank *La Maison de la Chimie* for the post-doctoral fellowship for SL.

Keywords: Lactam oximes • two-step one-pot cyclisation • Fmoc deprotection • amino-hydroxamic esters

- [1] S. J. Williams, R. Hoos, S. G. Withers *J. Am. Chem. Soc.* **2000**, *122*, 2223-2235
- [2] S. Numao, I. Damager, C. Li, T. M. Wrodnigg, A. Begum, C. M. Overall, G. D. Brayer, S. G. Withers *J. Biol. Chem.* **2004**, *279*, 48282-48291
- [3] R. Hoos, A. Vasella, K. Rupitz, S. G. Withers *Carbohydr. Res.* **1997**, *298*, 291-298
- [4] B. Ganem, G. Papandreou *J. Am. Chem. Soc.* **1991**, *113*, 8984-8985
- [5] T. V. Golovko, N. P. Solov'eva, O. S. Anisimova, V. G. Granik *Chem. Heterocycl. Compd.* **2003**, *39*, 344-353
- [6] B. Zacharie, N. Moreau, C. Dockendorff *J. Org. Chem.* **2001**, *66*, 5264-5265
- [7] Y. K. Chen, E. W. Co, P. Guntupalli, J. D. Lawson, W. R. L. Notz, J. A. Stafford, H.-T. Ton-Nu Oxim derivatives as HSP90 inhibitors. WO2009/097578, **2010**
- [8] B. Ganem, Y. Dong, Y. F. Zheng, G. D. Prestwich *J. Org. Chem.* **1999**, *64*, 5441-5446
- [9] B. N. Misra, A. S. Singha, G. S. Chauhan, R. Sharma *Indian J. Chem. Sect. B* **1984**, *23B*, 728-732
- [10] J. A. Smith, G. Le, E. D. Jones, J. Deadman *Future Med. Chem.* **2010**, *2*, 215-224
- [11] R. S. Roberts, S. Sevilla, M. Ferrer, J. Taltavull, B. Hernandez, V. Segarra, J. Gracia, M. D. Lehner, A. Gavaldà, M. Andres, J. Cabedo, D. Vilella, P. Eichhorn, E. Calama, C. Carcasona, M. Miralpeix *J. Med. Chem.* **2018**, *61*, 2472-2489
- [12] J. Wang, X. Wang, Y. Zhao, X. Ma, Y. Wan, Z. Chen, H. Chen, H. Gan, J. Li, L. Li, P. G. Wang, W. Zhao *MedChemComm* **2016**, *7*, 365-370
- [13] C. R. Groom, I. J. Bruno, M. P. Lightfoot, S. C. Ward *Acta Crystallogr. B Struct. Sci.* **2016**, *72*, 171-179
- [14] I. J. Bruno, J. C. Cole, M. Kessler, J. Luo, W. D. S. Motherwell, L. H. Purkis, B. R. Smith, R. Taylor, R. I. Cooper, S. E. Harris, A. G. Orpen *J. Chem. Inf. Comput. Sci.* **2004**, *44*, 2133-2144
- [15] P. W. Atkins, J. de Paula *Physical Chemistry*. 8th ed.; **2006**;
- [16] C. Reichardt, T. Welton Empirical Parameters of Solvent Polarity. In *Solvents and Solvent Effects in Organic Chemistry*, 4th edition ed., C. R. a. T. Welton, Ed. **2010**; pp. 425-508
- [17] R. Kumari, A. Varghese, L. George, Y. N. a. Sudhakar *RSC Adv.* **2017**, *7*, 24204-24214
- [18] G. B. Fields Methods for Removing the Fmoc Group. In *Peptide Synthesis Protocols*, M. W. Pennington; B. M. Dunn, Eds. Humana Press: Totowa, NJ, **1995**; pp. 17-27
- [19] M. Ueki, N. Nishigaki, H. Aoki, T. Tsurusaki, T. Katoh *Chem. Lett.* **1993**, *22*, 721-724
- [20] J. K. M. Agren, J. F. Billing, H. E. Grundberg, U. J. Nilsson *Synthesis* **2006**, 3141-3145
- [21] Bruker *Bruker AXS Inc., Madison, Wisconsin, USA* **2018**,
- [22] A. van der Lee *J. Appl. Crystallogr.* **2013**, *46*, 1306-1315
- [23] L. Palatinus, G. Chapuis *J. Appl. Crystallogr.* **2007**, *40*, 786-790
- [24] P. W. Betteridge, J. R. Carruthers, R. I. Cooper, K. Prout, D. J. Watkin *J. Appl. Crystallogr.* **2003**, *36*, 1487
- [25] R. I. Cooper, A. L. Thompson, D. J. Watkin *J. Appl. Crystallogr.* **2010**, *43*, 1100-1107

Entry for the Table of Contents



A one-pot deprotection/cyclisation synthesis was developed to access lactam oxime in mild condition. Reaction parameters were studied and after reaction optimisation, 5-, 6- and 7-membered ring lactam oxime were obtained.



Dr. Santiago Lascano received his Bachelor's and Master's degree at the University of Geneva, after which he obtained his PhD in 2016 in the group of Prof. S. Matile at the same university, working on orthogonal dynamic bonds for complex supramolecular systems. During his post-doctoral stay at the IBMM in Montpellier, he worked on synthesis of epigenetic modulators for anticancer treatments. Since 2019, he joined Syngenta as Process chemist.



Dr. Arie van der Lee graduated from the University of Groningen in experimental physics and completed there a doctoral thesis in 1992 on the properties of crystalline superionic materials. A postdoctoral study at the Institut des Matériaux de Nantes was focused on the structure determination of commensurately and incommensurately modulated inorganic compounds. At the Institut Européen des Membranes in Montpellier his expertise is in the field of thin film reflectometry and structure determination of inorganic and organic compounds by single-crystal and powder diffraction. He has had over the years a strong commitment within different national and international learned societies such as the International Union of Crystallography and the Association Française de Cristallographie. He is the current Vice President of the European Crystallographic Association.



Dr. Marie Lopez obtained her PhD in 2007 at Grenoble University working on chemo-enzymatic synthesis and interaction studies of oligosaccharides under the supervision of Dr. H. Driguez and Dr. A. Buléon. In 2010 she joined the Griffith Institute for Drug Discovery (GRIDD) in Brisbane she worked on glycosylated carbonic anhydrase inhibitors under the supervision of Prof. S.-A. Poulsen. She then worked on anti-infectious agents with Dr. S. Köhler (IRIM) and Prof. J.-Y. Winum (IBMM), in Montpellier. In 2013 she was recruited by the CNRS at the ETaC laboratory in Toulouse (headed by P. B. Arimondo) to work on targeting and understanding DNA methylation through inhibition and chemical probe strategies. In 2018 she moved to the IBMM in Montpellier, where she is managing projects in chemistry and chemical biology to understand and target epigenetic modifications in pathological contexts.